ELSEVIER

Marine and Petroleum Geology 18 (2001) 929–945

Marine and
Petroleum Geology

www.elsevier.com/locate/marpetgeo

Preferential mantle lithospheric extension under the South China margin

Peter Clift*, Jian Lin

Department of Geology and Geophysics, Woods Hole Oceanographic Institution, Woods Hole, MA 02543, USA

Received 27 November 2000; received in revised form 9 May 2001; accepted 9 June 2001

Abstract

Continental rifting in the South China Sea culminated in seafloor spreading at ~30 Ma (Late Oligocene). The basin and associated margins form a classic example of break-up in a relatively juvenile arc crust environment. In this study, we documented the timing, distribution and amount of extension in the crust and mantle lithosphere on the South China Margin during this process. Applying a one-dimensional backstripping modeling technique to drilling data from the Pearl River Mouth Basin (PRMB) and Beibu Gulf Basin, we calculated subsidence rates of the wells and examined the timing and amount of extension. Our results show that extension of the crust exceeded that in the mantle lithosphere under the South China Shelf, but that the two varied in phase, suggesting depth-dependent extension rather than a lithospheric-scale detachment. Estimates of total crustal extension derived in this way are similar to those measured by seismic refraction, indicating that isostatic compensation is close to being local. Extension in the Beibu Gulf appears to be more uniform with depth, a difference that we attribute to the different style of strain accommodation during continental break-up compared to intra-continental rifting. Extension in PRMB and South China slope continues for ~5 m.y. after the onset of seafloor spreading due to the weakness of the continental lithosphere. The timing of major extension is broadly mid-late Eocene to late Oligocene (~45–25 Ma), but is impossible to correlate in detail with poorly dated strike–slip deformation in the Red River Fault Zone.

Keywords: South China; Extension; Subsidence; Cenozoic

1. Introduction

Worldwide rifted margins have been classified into two apparently distinct classes: (a) non-volcanic margins, such as Iberia, Newfoundland and southern Australia, which are characterized by rotated basement fault blocks, wide zones of deformation extending more than 100 km from the continent–ocean transition (COT), and mantle peridotite exposures (e.g. Boillot, Beslier, Krawczyk, Rappin, & Reston, 1995); and (b) volcanic margins, such as East Greenland, Norway and NW Australia, with sharp COTs, voluminous subaerially erupted basalts, and thick bodies of gabbro underplated to the base of the original crust (e.g. Eldholm, Skogseid, Planke, & Gladczenko, 1995; Kelemen & Holbrook, 1995).

On non-volcanic margins, the nature of extension is still poorly understood, with debate continuing about whether simple or pure shear models are more appropriate in describing the deformation. On the Iberian continental margin, for example, low angle detachment faults have been invoked to explain the exposure of lower crust and upper mantle rocks close to the COT (e.g. Reston, Krawczyk, & Hoffman, 1995). Extension along non-volcanic margins has generally been viewed as an extreme end-member of the style of extension observed in intra-continental rift basins. However, in practice, the style of deformation recorded along rifted margins is often at odds with simple models for rift basins. Although the McKenzie (1978) model of crustal extension by pure shear explains much of the faulting and subsidence seen in intra-continental rifts such as the North Sea, the same cannot be said of the Early Cenozoic deformation associated with break-up in the nearby Northeast Atlantic. In this area, Cenozoic faulting is relatively modest, and contrasts with dramatic Cenozoic post-rift subsidence (Clift & Turner, 1998; Joy, 1992). These observations are incompatible with pure shear deformation, but might be explained by proposing that such a margin is on the 'upper plate' of a simple shear system, such as those found in the Basin and Range Province of western North America (Wernicke, 1985). Unfortunately, simple application of that model to rifted passive margins has lead to an upper plate interpretation being applied to opposing margins of the same basin, e.g. Galicia (Sibuet et al., 1995) and Newfoundland (Krawczyk & Reston, 1995). Direct application of the simple shear model does not appear to be appropriate

---

* Corresponding author. Tel.: +1-508-457-2000 ext. 3437; fax: +1-508-457-2187.

E-mail address: pclift@whoi.edu (P. Clift).

0264-8172/01/$ - see front matter
PII: S0264-8172(01)00037-X

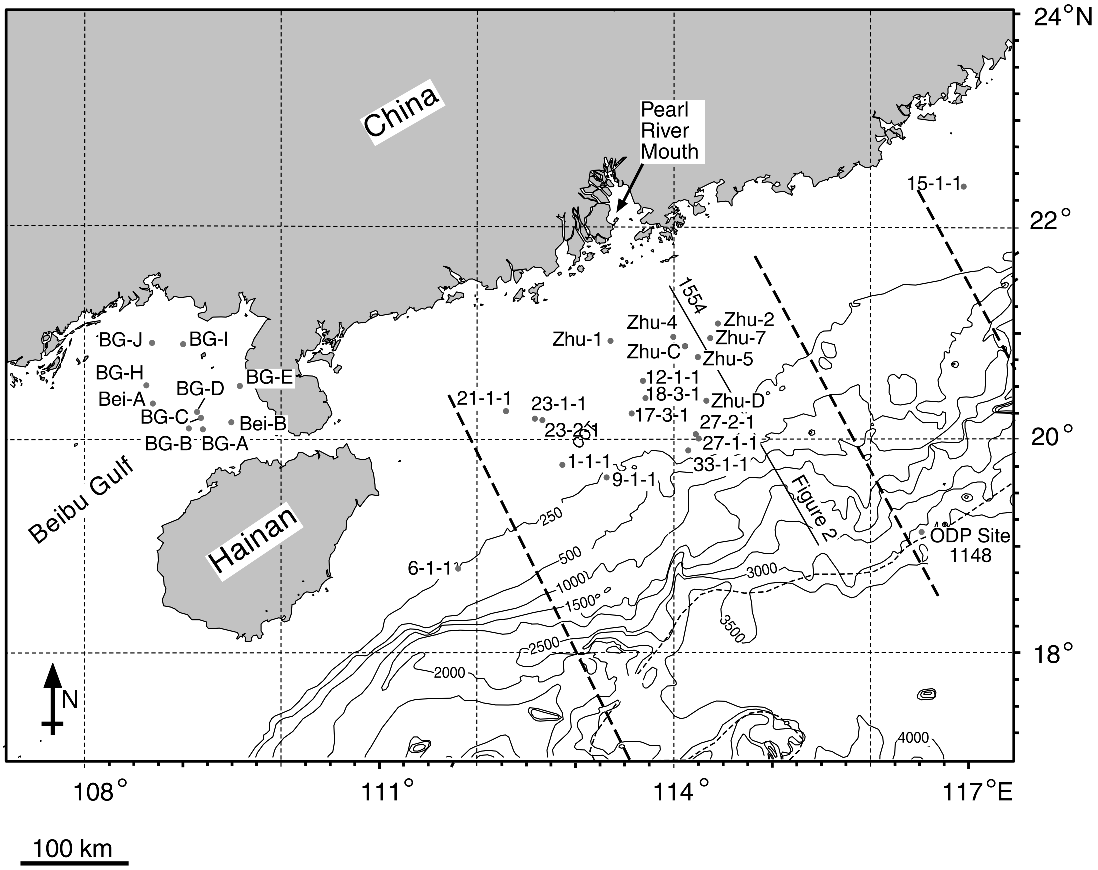

Fig. 1. Bathymetric map of the South China Shelf showing the location of the well sites considered in this study. Existing, deep-penetrating, seismic refraction profiles (Nissen et al., 1995a) are shown as dashed lines. Water depths in meters.

in the rifted margin environment (Driscoll & Karner, 1998).

In this paper, we document the timing, distribution and amount of extension in the crust and mantle lithosphere, respectively on the South China Shelf and in the adjacent Beibu Gulf Basin (Fig. 1). By doing so, we are able to examine the patterns of strain accommodation of similar crust in different extensional settings, intra-continental rift and passive margin. Documenting the age of extension furthermore allows the timing of deformation in the South China Sea to be understood in the context of associated tectonic events in East Asia.

2. Geologic setting

The South China Sea was formed by oceanic spreading along a WSW–ENE axis during the Oligo-Miocene (Briais, Patriat, & Tapponnier, 1993; Lu, Ke, Wu, Liu, & Lin, 1987; Taylor & Hayes, 1980). Extension in the area is believed to have started in the Late Cretaceous–Early Paleocene (Schlüter, Hinz, & Block, 1996), and seems to have exploited the location of a pre-existing Andean-type arc located above a north-dipping subduction zone along the south coast of China (Hamilton, 1979; Jahn, Chen, & Yen, 1976; Sewell & Campbell, 1997). Consequently, the lithosphere extended during formation of the South China Sea may have still been cooling towards an equilibrium state after the end of arc magmatism. Although U–Pb dating of the volcanic and intrusive rocks in Hong Kong (Davis, Sewell, & Campbell, 1997) indicate that magmatic activity ceased after 140 Ma, new ^{40}Ar/^{39}Ar ages of granites from the Pearl River Mouth Basin (PRMB) now suggest that some magmatism continued into the Late Cretaceous–Paleocene (Lee, Lo, Chung, Lan, Wang, & Lee, 1999). Thus, not more than ~80–90 m.y. of lithospheric cooling had occurred after the end of subduction, prior to the onset of extension. 80 m.y. is the time estimated for the continental lithosphere to regain thermal equilibrium (McKenzie, 1978). In this case, it is likely that rifting affected continental lithosphere that was hotter and weaker than equilibrium.

Propagation of oceanic spreading towards the WSW resulted in a V-shaped area of oceanic crust bounded to the east by an east-dipping subduction zone running N–S from the Philippine island of Mindoro to Taiwan, and to the west by the termination of the rift close to the southern end of Indochina. Extension prior to seafloor spreading increased towards the rift axis and resulted in a series of tilted fault blocks within a zone that would become the

COT. In addition, a series of sedimentary basins was generated, each separated from the main rift axis by blocks of less extended crust. The PRMB, which is the focus of this study, is the largest such basin on the northern margin of the South China Sea. Interpretation of magnetic anomalies places the start of seafloor spreading at ~30 Ma (anomaly 11) and finishing at ~16 Ma (Briais et al., 1993). Extension on the South China Margin appears to have ceased by 28 Ma (Clift, Lin, & ODP Leg 184 Scientific Party, 2001; Wang et al., 2000), shortly after the onset of seafloor spreading.

2.1. Origin of extension

It is still unclear what the driving mechanisms for the regional extension in the South China Sea are. In one set of models, the southern margin of the South China Sea (i.e. Dangerous Grounds, Reed Bank, North Palawan Block) would have been displaced southward relative to mainland China and Indochina along a major N–S trending transform zone near the Vietnam margin (e.g. Holloway, 1982; Liu, Wang, Yuan, & Su, 1985; Taylor & Hayes, 1983) during a phase of southward subduction under Borneo. Some influence has also been attributed to northward subduction beneath the Philippines, driving a backarc type of extension in the overriding plate (Taylor & Hayes, 1980). Wheeler and White (1997), however suggested that, because the crustal thicknesses derived from subsidence modeling of well dataand from gravity modeling were similar, then basin formation could be broadly considered as having been controlled by rift tectonics and that dynamically driven subsidence due to subduction (cf. Lithgow-Bertelloni & Gurnis, 1997) was not a factor in the South China Sea.

An alternative driving mechanism for extension favors southeastward lateral motion of Indochina and Borneo relative to a fixed China block (Peltzer & Tapponnier, 1988; Tapponnier, Peltzer, & Armijo, 1986). A variety of radiometric dating and paleomagnetic studies have attempted to test this theory (e.g. Burchfiel et al., 1997; Cung et al., 1998; Packham, 1996; Wang, Lo, Lee, Chung, & Yem, 1998), and although many recent studies indicate that the amount of offset during the time of South China Sea extension is insufficient to be the primary driving mechanism, the link between opening of the South China Sea and motion on the Red River Fault system remains controversial (e.g. Harrison, Leloup, Ryerson, Tapponnier, Lacassin, & Wenji, 1996; Leloup et al., 1993). Because the timing of India–Asia collision, the start of strike–slip faulting and the start of rifting are all poorly constrained, any proposed link is highly conjectural.

Whatever the extension-driving mechanism, it is clear that rifting of the South China margin is linked to the Late Oligocene propagation of an oceanic spreading center between two continental areas, the South China margin and the conjugate Dangerous Grounds/Palawan margin. The passive margin sediments that accumulated during the rifting process are best studied in the PRMB, where they have been sampled by numerous petroleum exploration wells. The eastern South China Sea appears to have started spreading during Chron 11 time (30 Ma; Briais et al., 1993), with clearer propagating geometry further towards the SW. Thus, we may consider the timing of extension and seafloor spreading adjacent to the PRMB to be effectively synchronous along its length.

The sediments of the PRMB are typically continental, alluvial at the base, and show a deepening upward into shelf siliciclastic sediments. Detailed biostratigraphic work coupled with lithologic variation has allowed the subdivision of the section into nine separate formations (Su, White & Mckenzie, 1989), whose exact definition is not important to the analysis presented here. Thin Maastrichtian sediments are present locally, succeeded by continental alluvial Paleocene to Early Eocene siltstones and sandstones. From Early to Middle Eocene, dark lacustrine shales were deposited, followed by Early Oligocene coal-bearing swamp and littoral plain sediments. Soon after the major extensional episode during the Eocene–Oligocene, sedimentation became submarine throughout the basin. Recent drilling at Ocean Drilling Program (ODP) Site 1148 near the COT (Fig. 1) revealed bathyal syn-rift sedimentation during the Late Oligocene (Wang et al., 2000). Drilling on the Reed Bank identified deep-water, clastic sedimentary rocks of pre-Middle Eocene age (Taylor & Hayes, 1980), indicating that there was significant pre-rift relief along a N–S axis.

2.2. Age control

Much of the sediment deposited on the shelf today is derived from the Pearl River in the central part of the shelf, or from the Red River in the westernmost areas, although it seems likely that other larger rivers fed sediment into the sea during the Cenozoic (Clift, Clark, Royden, Burchfiel, & Whipple, 2000). Dating of the sediments is well-constrained following marine transgression in the Early Oligocene. Earlier ages within the syn-rift deposits, however, are generally determined by palynological methods, which provide a poorly defined Eocene–Oligocene age. Consequently, the start and duration of the syn-rift episode are not rigidly defined. The best date for the end of active extension now comes from ODP Site 1148 on the continental slope offshore the PRMB. Although the start of rifting is not constrained here, reflection seismic and sediment accumulation rate data suggest that active extension, at least adjacent to the COT, was complete by ~28 Ma (Wang et al., 2000).

3. Data sources

The subsidence analysis performed in this study is based on well data from across the South China Shelf and Beibu Gulf (Fig. 1). These data were released for research by agreement with the Chinese National Offshore Oil

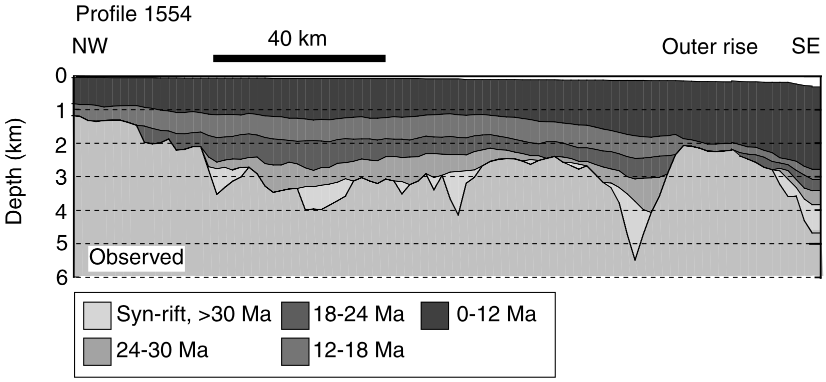

Fig. 2. Cross section through the PRMB in the region of densest well coverage, showing the well developed shelf basin separated from the slope by a major structural high.

Company (CNOOC) and BP (BP Exploration Operating). A single multichannel seismic profile is provided here to demonstrate the overall structure of the PRMB in the region of greatest well coverage (Fig. 2). The most notable feature is the presence of a large structural high between the PRMB and the outer continental slope. The profile was interpreted from a 96-channel seismic reflection survey that covers the entire continental shelf.

The stratigraphy on the South China margin is constrained by 30 wells for which lithologic and biostratigraphic data was also released. Twenty-one of the wells penetrated to crystalline basement, while the remainder bottoming in syn-rift alluvial clastic sediments of Eocene–Oligocene age. Results from four wells, Bei-A, Bei-B, Zhu-5 and Zhu-7, are derived from the work of Su et al. (1989), and eight others located in the Beibu Gulf Basin west of Hainan Island (Fig. 1) from the study of Webb (1992). The original well data were not available from these 12 wells. When determining ages for the subsidence analysis described below, we follow the time scale of Berggren, Kent, Swisher and Aubry (1995), using the nannofossil and foraminiferal zone determinations from well logs at each of the sites considered.

4. Subsidence analysis of well data

The drilled section at 30 wells on the South China Shelf provides a unique data set from which tectonically induced subsidence of the basement can be quantified by the traditional one-dimensional backstripping method. The residual subsidence history of the basement, which is obtained after correcting for the loading effect of the sedimentary overburden, reflects different stages of the rifting process (Sclater & Christie, 1980). Syn-rift subsidence represents the difference between the basement subsidence due to crustal thinning and uplift due to lithospheric mantle thinning (Royden & Keen, 1980). In contrast, the post-rift thermal subsidence generally reflects only the cooling and thickening of the mantle lithosphere, although in cases of high extension, heating and cooling of the lower crust may also be a significant factor in driving post-rift subsidence. By isolating and quantifying the amount of syn-rift and post-rift subsidence respectively, estimates can be made of both the mantle and whole crustal extension factors (Royden & Keen, 1980).

A numerical backstripping method was used by which the vertical motion of the basement at a given drill site was tracked through time, while accounting for the loading effects of sediment, as well as fluctuations in the global eustatic sealevel (Sclater & Christie, 1980). The second order sealevel reconstruction of Haq, Hardenbol and Vail (1987) was used, despite ongoing controversy related to the timing and especially magnitude of sealevel fluctuations. Sealevel variability determined from isotopic studies (e.g. Miller, Mountain, & Tucholke, 1985) is only about one third of the magnitude estimated from sequence stratigraphy by Haq et al. (1987). Consequently, our reconstruction may overestimate the influence of falling sealevels, which would result in overestimates of the amount of tectonic subsidence. Because this change is over a long time period, a poor correction for sealevel will affect the estimate of the post-rift thermal subsidence more than the short-lived syn-rift subsidence. The result of using Haq et al.'s (1987) reconstruction may be to overestimate the amount of mantle extension, which is the primary control on thermal subsidence. Since mantle lithosphere extension alone produces syn-rift uplift, the amount of crustal extension estimated will also increase because additional extension will be needed to balance the mantle driven uplift and match the total amount of subsidence observed. The net effect of a poor sealevel correction is to increase extension but not to influence the relative amounts of crustal versus mantle extension.

Although water depth is accounted for in the analysis, the basement at each well is not unloaded for water. Reconstructions are presented as water-filled basins in order to allow direct comparison with the models of McKenzie (1978) and Royden and Keen (1980). The input data were lithology, age, and paleo-water depth, all of which were

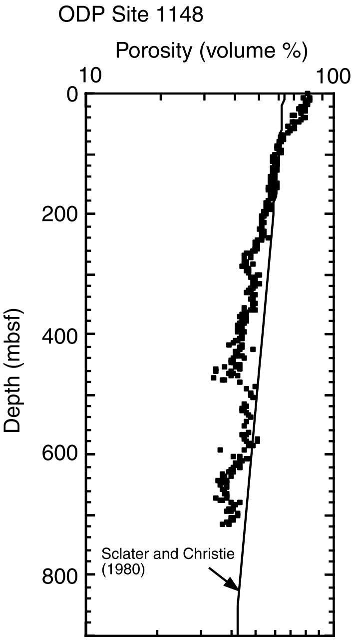

Fig. 3. Comparison of in situ sediment porosity determined by borehole geophysical logging methods at ODP Site 1148 (Wang et al., 2000) compared to the model prediction of Sclater and Christie (1980) based on data from wells in the North Sea.

estimated by CNOOC and BP contractors and recorded on standard oil industry well logs. There is no reason to suppose that the quality of these data is poor, although these data cannot be readily verified. Each log provides an array of foraminifer and nannofossil, and sometimes palynological biostratigraphic data and was converted to a numerical age using the scheme of Berggren et al. (1995). The greatest uncertainties lie in the use of palynology for the predominantly continental syn-rift sediments, where nannofossils and foraminifers are absent. The age assignments based on these are often poor and consequently the duration of rifting is often not well constrained. Since marine transgression occurred quickly after break-up, the age of the end of rifting is best known.

The physical parameters of each sediment type, in terms of density, porosity and compaction characteristics, were taken from Sclater and Christie (1980), based on measurements from the North Sea basin. Although there is only modest variability in the compaction of sandstones with depth, shales may depart significantly from the predictions, especially at shallow depths and if they become overpressured (Falvey & Middleton, 1981). Fortunately, in situ borehole geophysical logging data from ODP Site 1148 on the South China slope now show that the muddy sediments in this region do follow closely the compaction history predicted by Sclater and Christie (1980). Fig. 3 shows that the only significant deviation between porosity data and model are in the thin uppermost stratigraphic levels and at the level of the break-up unconformity in Hole 1148A (Wang et al., 2000). In the latter case, the discrepancy is related to the presence of deformation below the unconformity and to an unusual major slump unit overlying. Under normal burial conditions, the sediments of the South China margin appear to follow the Sclater and Christie (1980) model closely.

4.1. Isostatic equilibrium

The one-dimensional backstripping method developed by Sclater and Christie (1980) assumes local isostatic compensation that is a reasonable approximation only where the lithosphere is weak, or where the applied sediment load is widely and evenly distributed. Studies of extensional sedimentary basins such as the North Sea (e.g. Barton & Wood, 1984) have indicated that the lithosphere beneath sedimentary basins is very weak (effective elastic thickness <5 km) during the rifting and early post-rift period. Karner and Watts (1982) showed that the rifted continental crust of the Coral Sea and Lord Howe Rise still only has an elastic thickness of 5 km, even though rifting was completed at 60 Ma. In a backstripping and forward modeling study of the Gabon passive margin of west Africa, Watts and Stewart (1998) demonstrated that low effective elastic thicknesses ($T_e < 10$ km) provided the best match to the observed stratigraphy during the rift and early post-rift periods. Thus it is likely that a young passive margin such as South China had and still retains a low flexural rigidity.

Data from South China Sea now show that this area is also weak and consistent with other rifted margins. Seismicity under the South China Shelf is now shallower than ~15 km (Harvard Catalogue), again suggestive of low strength (ductile rheology) in the lower crust and mantle lithosphere (Maggi, Jackson, McKenzie, & Priestley, 2000), contrasting with strong cratons with deep earthquakes and high T_e (Foster & Jackson, 1998). Although flexural rigidity measurements in the East Africa rift show much higher T_e (Ebinger, Bechtel, Forsyth, & Bowin, 1989; Petit & Ebinger, 2000), this system located within a craton is an inappropriate analogue to an arc rift setting. South China Sea is likely more similar to the modern Gulf of California or the Woodlark Basin. The Maastrichtian–Paleocene magmatism under the PRMB that shortly pre-dates rifting (Lee et al., 1999) require that the lithosphere would have

Fig. 4. Sediment-unloaded, tectonic subsidence reconstructions for the basement of the South China Shelf at a series of petroleum exploration wells. Basement depths are calculated using the backstripping routine of Sclater and Christie (1980). Vertical heights of the bars show the uncertainties in the paleo-water depth of deposition. Poorly constrained age assignments, usually palynology-derived, are marked by question marks. Gray-shaded regions show the interpreted active rift periods. Vertical dashed lines are epoch boundaries from the timescale of Berggren et al. (1995). All wells penetrate to pre-rift crystalline basement unless marked 'Basement not penetrated'.

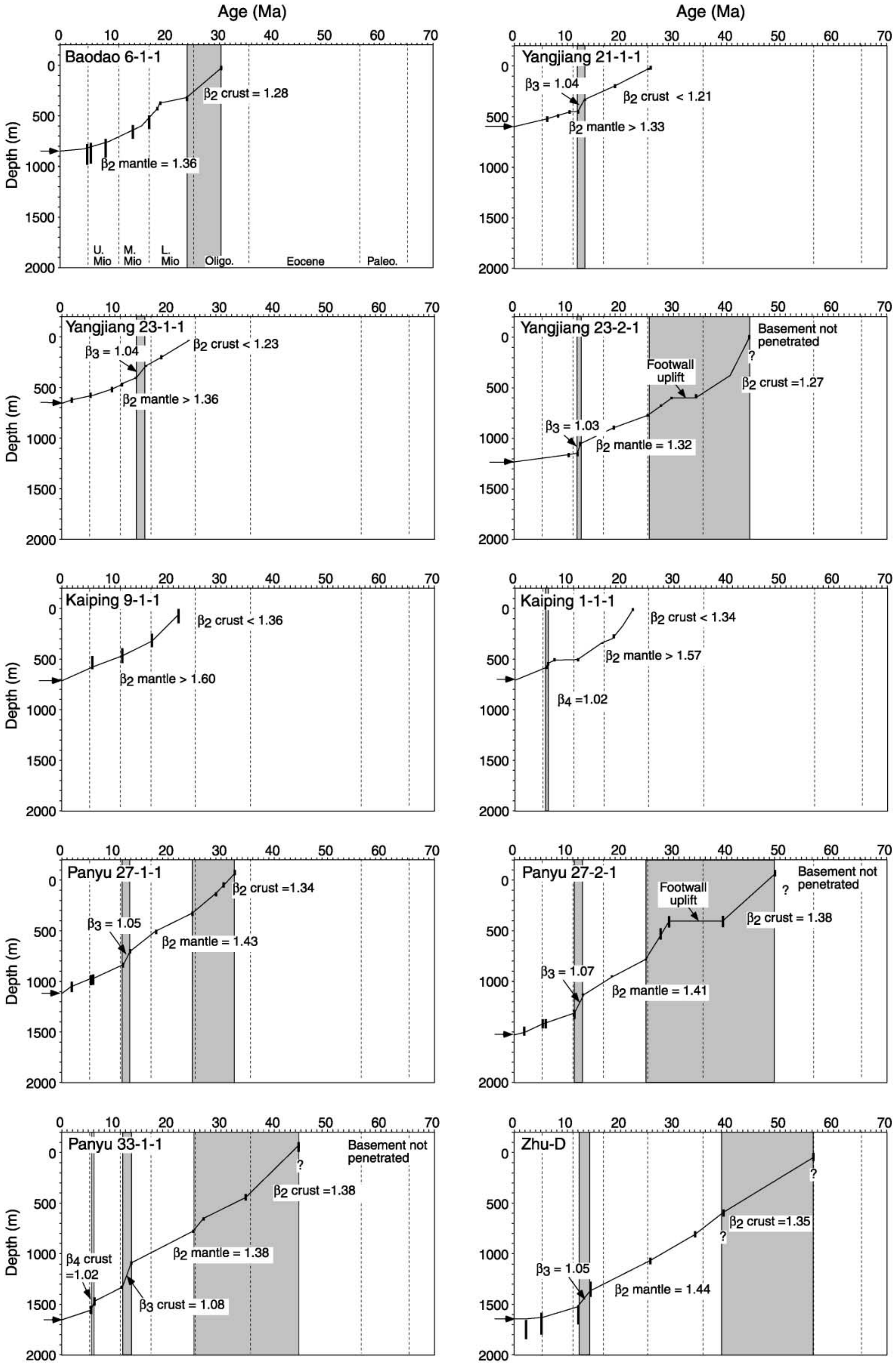
Age (Ma)
Depth (m)
Baodao 6-1-1
β2 crust = 1.28
β2 mantle = 1.36
U. Mio
M. Mio
L. Mio
Oligo.
Eocene
Paleo.
Yangjiang 21-1-1
β3 = 1.04
β2 crust < 1.21
β2 mantle > 1.33
Yangjiang 23-1-1
β3 = 1.04
β2 crust < 1.23
β2 mantle > 1.36
Yangjiang 23-2-1
Basement not penetrated
?
Footwall uplift
β2 crust =1.27
β3 = 1.03
β2 mantle = 1.32
Kaiping 9-1-1
β2 crust < 1.36
β2 mantle > 1.60
Kaiping 1-1-1
β2 crust < 1.34
β2 mantle > 1.57
β4 =1.02
Panyu 27-1-1
β2 crust =1.34
β3 = 1.05
β2 mantle = 1.43
Panyu 27-2-1
Basement not penetrated
?
Footwall uplift
β2 crust = 1.38
β3 = 1.07
β2 mantle = 1.41
Panyu 33-1-1
Basement not penetrated
?
β2 crust =1.38
β2 mantle = 1.38
β4 crust =1.02
β3 crust = 1.08
Zhu-D
?
β2 crust =1.35
?
β3 = 1.05
β2 mantle = 1.44
0
10
20
30
40
50
60
70
0
500
1000
1500
2000

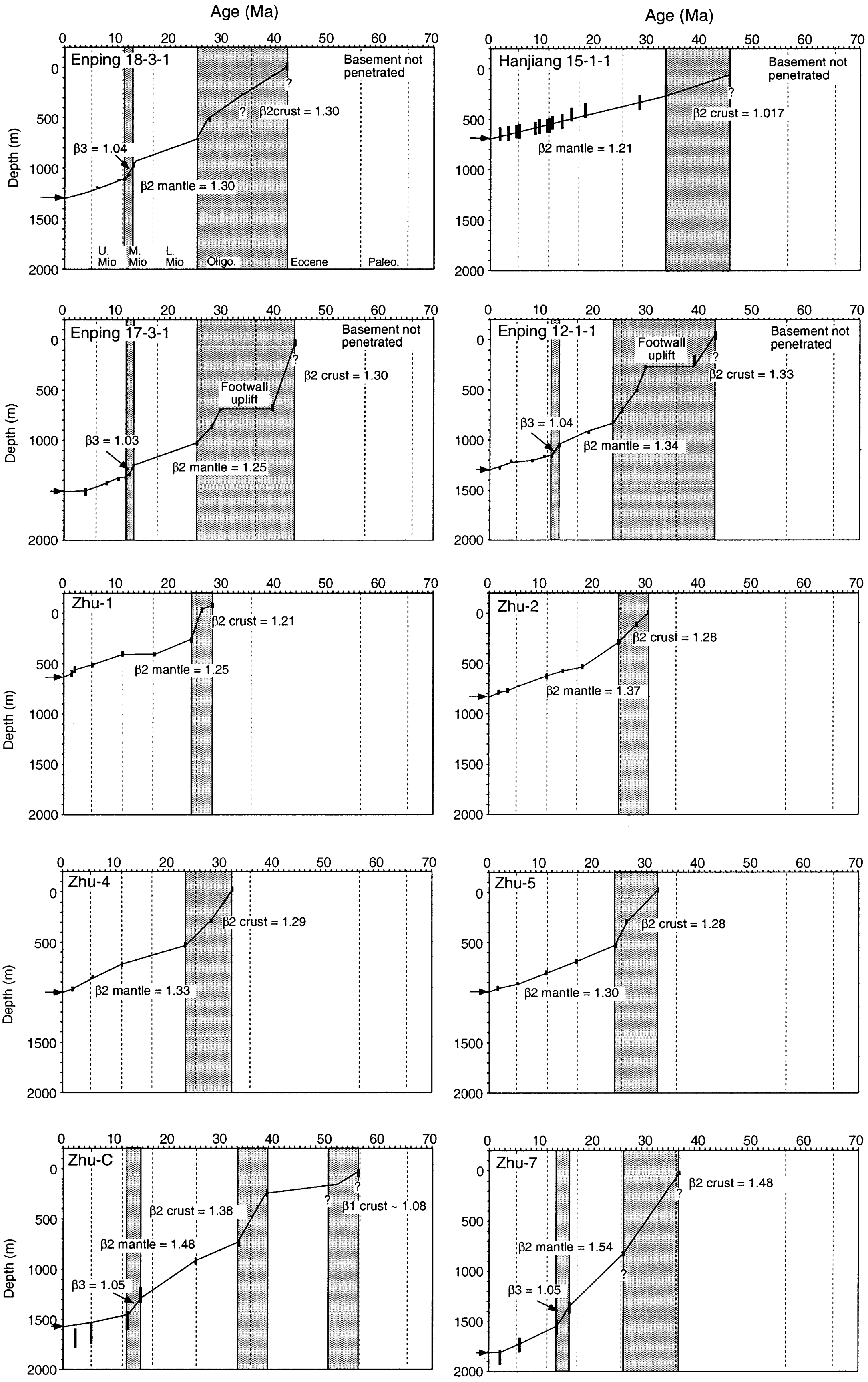

Fig. 4. (*continued*)

been thermally young and weak during Oligocene break-up. Furthermore, although the upper mantle is generally strong in oceanic lithosphere, in continental arc settings, it is likely to be very weak because of the abundance of water, whose presence would be expected to dramatically lower the viscosity and thus strength (Hirth & Kolhstedt, 1996). The total effect is to concentrate strength in the South China margin upper crust, closely approximating the local isostatic balance required by the one-dimensional method.

Two dimensional flexural modeling of the subsidence in the PRMB has demonstrated that flexural rigidity during rifting must have been low to account for the narrow and deep geometries of the sub-basins within the shelf (Fig. 2). T_e estimates of 5 km or less were found most appropriate for modeling these basins (Clift et al., 2001). One important conclusion derived from the two dimensional modeling was that extension of the crust was strongly partitioned between the brittle faulted upper crust and a ductile lower crust, that was preferentially lost. Consequently, measuring extension across seismically imaged faults is not a good measure of total crustal extension, which must rather be derived from the accommodation space created. Drilled sections are an effective way of accurately measuring this space. The detachment between lower and upper crust contrasts with the situation in rifts located within cratonic lithosphere where anomalies between subsidence predicted from faulting and that measured in structural profiles is negligible (e.g. Gulf of Suez; Steckler, Berthelot, Lyberis, & Le Pichon, 1988).

4.2. Paleo-water depths

Estimates of paleo-water depth are often a significant source of uncertainty when attempting backstripping subsidence analysis. On the South China shelf, however, most of the wells now lie in around 100 m of water. Well logs show continental or shallow marine facies throughout the column, constraining water depths to no more than 200 m, since the end of rifting. Uncertainties in the elevation of continental sediments are higher because there is no upper bound known. However, comparison with modern rift systems (e.g. Gulf of Suez, Gulf of Corinth) suggests that the elevation of syn-rift basins is rarely more than ~200 m above sealevel, a suggestion supported by the transgression of marine sediments over even the fault block highs shortly after the end of extension (see below). With such high resolution data, the uncertainties introduced from this source are minor in sediment columns typically 2–3 km thick, thus allowing the restored level of the basement to be accurately determined.

5. Results of backstripping

The results of the backstripping analysis are shown in Fig. 4 (South China Shelf) and Fig. 5 (Beibu Gulf). The interpreted crust and mantle extension factors are presented in Tables 1 and 2, respectively. At each well, the subsidence history was split into a number of discrete extensional events, marked by a significant steepening of the tectonic subsidence rate. Extension of the continental crust results in short-lived, often rapid syn-rift subsidence and a longer lasting increase in the rate of the thermal subsidence. Provided the age resolution of the stratigraphy is sufficient, these events should be apparent in the reconstructed basement subsidence history, if they are not clear from the seismic profiles through the well sites. Syn-rift sequences identified in seismic profiles (Fig. 2) show a fanning pattern against the active fault scarp. In order to highlight changes in the rate of tectonic subsidence, we join each dated subsidence control point at its mid point to provide a visual image of the vertical motion of the basement through time (Figs. 4 and 5).

Table 1
1-D backstripping results from wells in the PRMB

South China Shelf wells	Oligocene		Mid Miocene	
	$\beta 2$ Crust	$\beta 2$ Mantle	$\beta 3$ Crust	$\beta 3$ Mantle
Baodao 6-1-1	1.28	1.36	–	–
Yangjiang 21-1-1	<1.21	>1.33	1.04	1.04
Yangjiang 23-1-1	<1.23	>1.36	1.04	1.04
Yangjiang 23-2-1	1.27	1.32	1.03	1.03
Kaiping 9-1-1	<1.36	1.6	–	–
Kaiping 1-1-1	<1.34	>1.57	–	–
Panyu 27-1-1	1.34	1.43	1.05	1.05
Panyu 27-2-1	1.38	1.41	1.07	1.07
Panyu 33-1-1	1.38	1.38	1.08	1.08
Zhu D	1.35	1.44	1.05	1.05
Enping 18-3-1	1.30	1.30	1.04	1.04
Hanjiang 15-1-1	1.02	1.21	–	–
Enping 17-3-1	1.30	1.25	1.03	1.03
Enping 12-1-1	1.33	1.34	1.04	1.04
Zhu-1	1.21	1.25	–	–
Zhu-2	1.28	1.37	–	–
Zhu-4	1.29	1.33	–	–
Zhu-5	1.28	1.30	–	–
Zhu-C	1.38	1.48	1.05	1.05
Zhu-7	1.48	1.54	1.05	1.05

Table 2
1-D backstripping results from wells in the Beibu Gulf

Beibu Gulf wells	Paleocene–Eocene		Oligocene	
	$\beta 1$ Crust	$\beta 1$ Mantle	$\beta 2$ Crust	$\beta 2$ Mantle
Bei-A	1.31	1.31	–	–
Bei-B	1.35	1.37	–	–
BG-A	1.36	1.36	1.24	1.23
BG-B	–	–	1.17	1.19
BG-C	–	–	1.43	1.43
BG-D	–	–	1.21	1.25
BG-E	1.1	1.1	1.29	1.21
BG-H	–	–	1.45	1.61
BG-I	–	–	1.235	1.27
BG-J	1.24	1.3	1.09	1.06

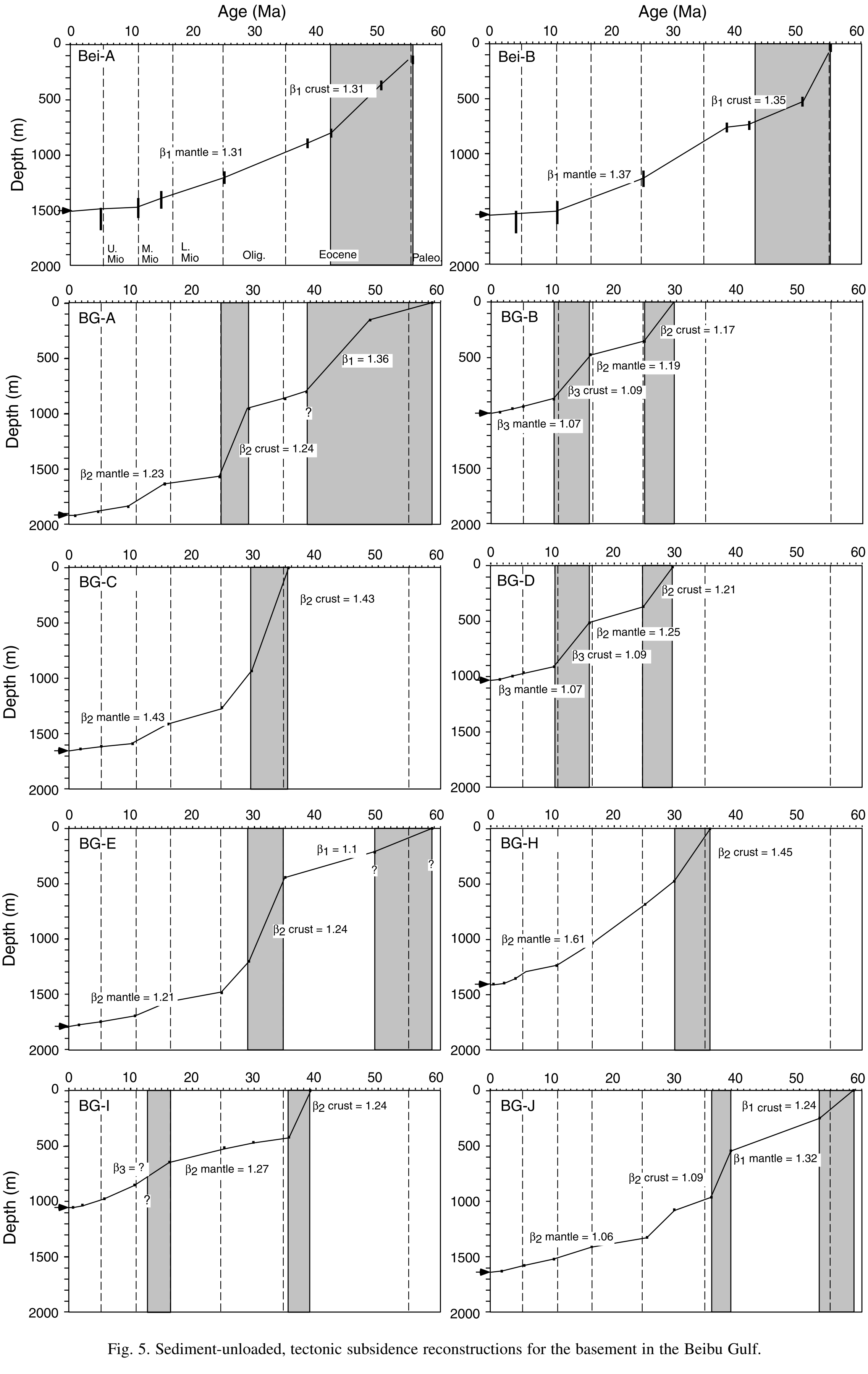

Fig. 5. Sediment-unloaded, tectonic subsidence reconstructions for the basement in the Beibu Gulf.

For most wells on the South China Shelf, three rifting episodes are noted at 45–55, 45–25 and ~12–14 Ma, with the second being generally the larger. At two wells Kaiping 1-1-1 and Panyu 33-1-1, an additional event at 5 Ma was recognized. In Beibu Gulf, the extensional event at 55 Ma is seen to dominate. Due to the poor dating of syn-rift deposits, it is not possible to demonstrate a time transgressive nature to the rifting, which may have been synchronous along the margin. Rifting was mostly completed by 25 Ma in the PRMB, shortly after the proposed onset of seafloor spreading in the adjacent basin (Briais et al., 1993), and close to the inferred 28 Ma break-up unconformity at ODP Site 1148 (Clift et al., 2001). Extension in the Beibu Gulf also appears to have continued at least locally until ~25 Ma. Following the cessation of spreading at ~16 Ma, the margin experienced a later minor extensional phase ($\beta = 1.03 - 1.08$) that caused some reactivation of older fault lineaments, and a small amount of subsidence, recorded as a minor increase in the rate of basement subsidence at ~12–14 Ma. Localized minor deformation starting at 5 Ma may extend to the present day, manifest as slight offsets of the seafloor by reactivated faults.

5.1. Estimating mantle extension

Because we are trying to assess the applicability of simple versus pure shear models for margin extension, we cannot assume that crustal and lithospheric mantle extension are equal (cf. McKenzie, 1978). Instead, we shall determine whether uniform extension is appropriate by independently determining crustal and mantle extension. Mantle extension beneath each well is estimated from the equations of McKenzie (1978) based on the rate of tectonic subsidence after the cessation of active rifting. Models of instantaneous extension predict a significant slowing in the rate of subsidence at the end of active rifting, which may be recognized on reconstructed subsidence histories or from interpretation of growth faulting on seismic profiles. On the subsidence reconstructions presented in Figs. 4 and 5, each extensional event is numbered 1, 2, 3 or 4. We denote event 1 to be rifting during the Paleocene–Eocene, event 2 in the Eocene–Oligocene, event 3 in the mid Miocene, and event 4 to be late Miocene–Pliocene. Where seismic data is lacking and no strong changes in subsidence rates are apparent, then the division between syn-rift and post-rift periods is likely to be subjective. This is probably the single greatest uncertainty encountered in estimating mantle extension.

Interpretation of reconstructed subsidence histories in terms of an instantaneous rift episode is clearly only an approximation, given that the observed syn-rift sedimentation probably continued for 10–15 m.y. Jarvis and McKenzie (1980) demonstrated, however, that for rifting events of duration less than 20 m.y., the assumption of an instantaneous rifting event does not introduce significant errors into the calculation of mantle extension from the post-rift subsidence. In any case, since the duration of extension is only poorly known from the palynology of the syn-rift sediments, it is simply not feasible to accurately correct for lithospheric cooling during active extension. Consequently, this approximation was used in determining extension factors. In practice, this assumption has yielded results that are compatible with other independent data sets (e.g. igneous geochemistry, seismic refraction data). As noted below, total crustal extension estimates from the PRMB are close to those determined by seismic refraction methods (Nissen, Hayes, Bochu, Weijun, Yongqin, & Xiaupin, 1995a,b).

Fig. 6 shows an idealized subsidence history to demonstrate how the amount of mantle extension is determined. In the case of simple one stage extension, the degree of mantle lithospheric thinning is derived from the amount of subsidence (h_2) that has occurred in time T_2 since the cessation of active extension. The amount of subsidence during active extension (h_1) is controlled by both mantle and crustal extension. The degree of crustal extension can be extracted once the mantle extension has been determined from the amount of post-rift subsidence. In the case of two or more rifting events (Fig. 6(B)), the amount of mantle extension in the first event is calculated in the same fashion, i.e. from the amount of subsidence (h_2) that has occurred in time T_2. However, the amount subsidence that occurs following the second rift event reflects not only the subsidence induced by extension during that second event, but also residual mantle thinning from the first event. Thus the amount of mantle extension during the second rift event reflects the amount of extra subsidence, $h_5 - h_3$ (i.e. the difference between the total amount of thermal subsidence following the end of the second rifting event and the amount of thermal subsidence that would be predicted to have occurred during that period if the second event had not occurred), recorded during time T_4 (Fig. 6(B)).

5.2. Estimating crustal extension

The crustal extension during any given extensional event can be determined through quantifying the total amount of subsidence during the syn-rift period, assuming instantaneous rifting. We also assume that all post-rift subsidence is thermally driven, following the models of McKenzie (1978) and Royden and Keen (1980). In the simple, single stage extension example (Fig. 6(A)) the amount of syn-rift subsidence (h_1) reflects the net effect of subsidence due to crustal thinning and a local, instantaneous isostatic response and uplift due to thinning of the dense mantle lithospheric root. Because the amount of mantle lithospheric extension can be estimated from the rate of post-rift thermal subsidence, as shown in Section 5.1, we can estimate the amount of uplift that this would have caused at the time of rifting. Consequently, the difference between the predicted uplift and the measured subsidence must be caused by crustal extension, which can then be estimated

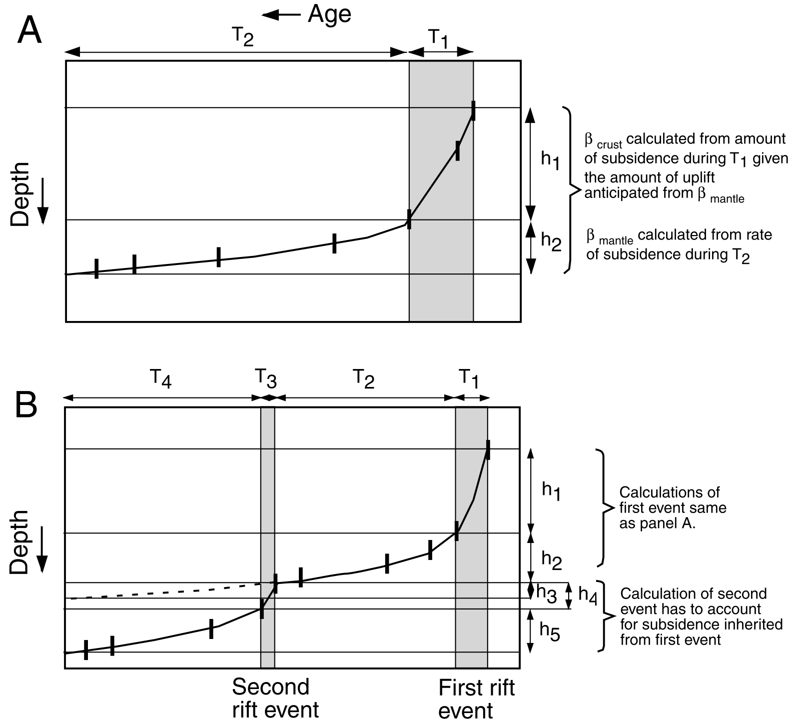

Fig. 6. Schematic subsidence reconstruction showing how the mantle and crustal extension factors are calculated for: (A) a single rifting event, and (B) in the case of a second event.

by assuming local isostatic equilibrium. In cases where extension follows an earlier extensional event (Fig. 6(B)), the additional mantle extension is calculated in the manner discussed above, and the same procedure is repeated using the observed syn-rift subsidence during the second event (h_4).

5.3. Middle Miocene extension

Water depth estimates are a minor concern in estimating crustal extension on the South China Shelf for the Oligocene, but are significant for the Mid Miocene (event 3: ~12–14 Ma) and for the Late Miocene–Pliocene (event 4; ~5 Ma). The subsidence reconstructions normally show event 3 to be associated with a drop in unloaded basement level of 100–200 m, similar to the degree of water depth uncertainty. As a result, the uncertainty in estimating extension during event 3 is large, although we can confidently constrain the maximum extension to be small, <10%. The same is true of event 4, where the amount of subsidence is even smaller and extension can only be loosely defined as being close to 2% at Kaiping 1-1-1 and Panyu 33-1-1 (Fig. 1). The slight increases in thermal subsidence rate caused by events 3 and 4 are beyond the resolution of the water depth uncertainties, so that the mantle extension cannot be meaningfully estimated. Consequently, we opt to treat events 3 and 4 as a uniform extension episodes, whose magnitude is estimated solely from the amount of syn-rift subsidence.

5.4. Interpretation of structural setting

When interpreting the reconstructed subsidence histories for each well, it is necessary to consider its structural position because wells situated on the hanging wall of a fault block will tend to show more syn-rift sedimentation than those on the footwall (Sawyer, 1986). Even when flexural rigidity is low, it has been shown that faulting will have significant effect on the sedimentation history at a given site (e.g. Kusznir & Egan, 1989), in contrast to the simplified pure shear model of McKenzie (1978). On the other hand, post-rift thermal subsidence will tend to be similar for wells on the footwall and hanging wall because the mantle lithosphere deforms over long wavelengths.

Drilling at Panyu 27-1-1 and 27-2-1 (Fig. 1) shows that, despite being situated close together, these wells have quite different stratigraphies and thus reconstructed subsidence histories. Panyu 27-1-1 is located on the footwall of an apparent normal fault and has only accumulated post-rift sediments since ~25 Ma. In contrast, well Panyu 27-2-1 is located on the edge of the hanging wall and penetrates some, but not the maximum thickness, of the syn-rift stratigraphy (Fig. 7). The basal part of the section drilled at Panyu 27-2-1 has been lost due to faulting. The hiatus at Panyu 27-1-1 during rifting may reflect subaerial erosion at that time followed by transgression after the cessation of extension. The post-rift period at Panyu 27-1-1 is not preserved in its entirety because of the finite period of time between the end of rifting and transgression of the

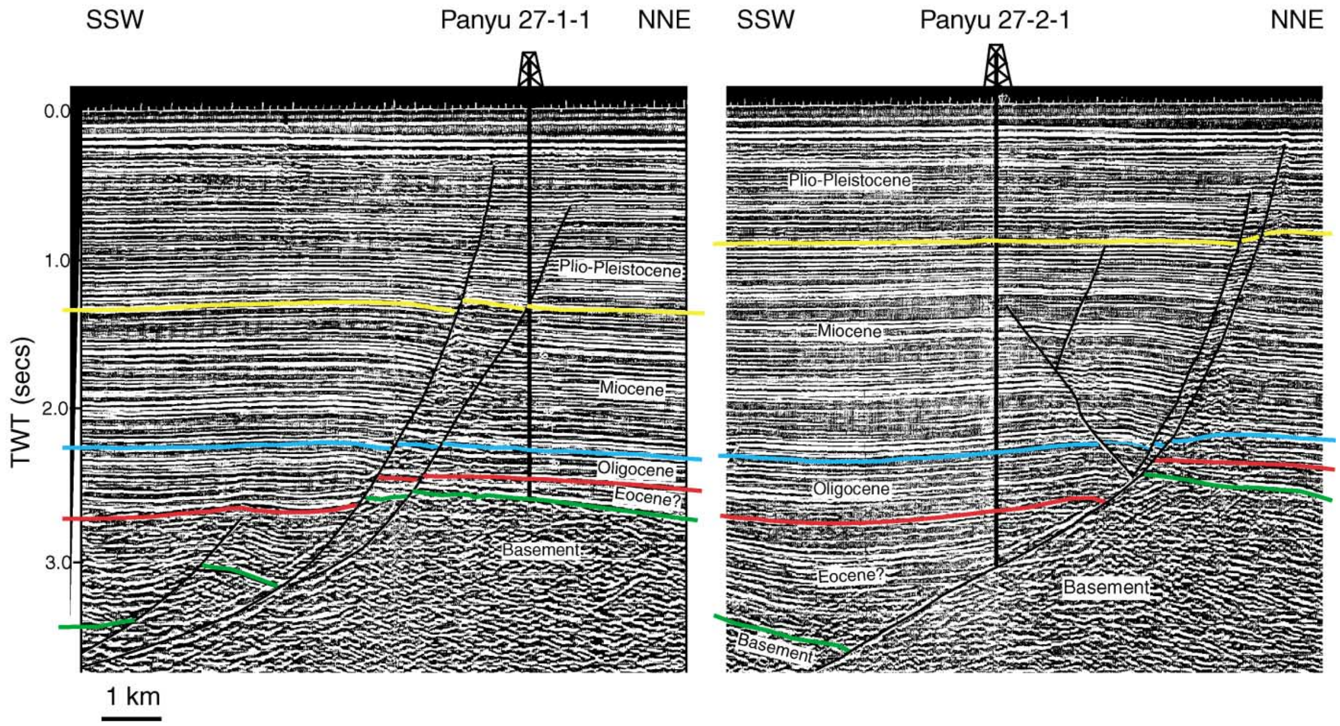

Fig. 7. Interpreted cross sections of multichannel reflection seismic data at the location of wells Panyu 27-1-1 and 27-2-1. Panyu 27-1-1 is located on the footwall to a major normal fault so that the well does not penetrate syn-rift sediment. In contrast, well 27-2-1, which is located off the crest of the fault block does cut some of the interpreted Eocene–Oligocene syn-rift.

fault block, although this is short. Thus, estimates of the mantle extension based on the rate of post-rift subsidence at Panyu 27-1-1 will tend to underestimate the degree of extension because the record of the earliest and most rapid phase of subsidence is missing. However, the well, like many on the South China margin, penetrated pre-rift crystalline basement, so that no errors are introduced due to compaction of sediment beneath the base of the drilled section. Seismic data suggests that, although Panyu 27-2-1 did not penetrate basement, it did sample a significant part of the section. Fig. 7 shows that a complete syn-rift section is located away from the fault that cuts out the basal part below the drilled section. If this complete section had been drilled, then a higher value for crustal extension would have been derived. Seismic data demonstrate that very little of the post-rift cover seen at Panyu 27-2-1 is missing at 27-1-1 (Fig. 7), so that the estimate of mantle extension derived from the preserved cover is close to the real value.

The observation that the tops of fault blocks are submerged soon after the end of active rifting if an important one. It demonstrates that none of the rift system was elevated far above sealevel during active deformation. The fact that the syn-rift fill in the basin was continental and was then transgressed just before the adjacent fault blocks and just after the end of active extension suggests that the rift basins were almost full of sediment at that time. This is important because the method of estimating crustal extension described above is principally dependant on the thickness of the syn-rift section. Unfilled accommodation space would lead to significant underestimates of crustal extension, but the seismic data indicate that this is not likely to be a major issue in the PRMB, especially for those basins close to the coast. The same is not true for the continental slope.

A minimum value of mantle extension during event 2 at Panyu 27-1-1 can be established at $\beta_{\mathrm{mantle}} = 1.43$, where β is defined by the ratio of mantle thickness prior to extension to that after extension. This value is somewhat less than, but consistent with, the peak values of $\beta_{\mathrm{mantle}} = 1.8$ reported by Su et al. (1989) for a pseudo-well in the basin center, i.e. one that does take into account the full syn-rift sequence. The β_{mantle} estimate in turn can be used to estimate a maximum value of crustal extension at $\beta_{\mathrm{crust}} = 1.34$, based on the degree of extension needed to provide a space for the preserved volume of syn-rift sediment. The subaerial exposure at Panyu 27-1-1 implies that the uplift generated by mantle thinning and footwall uplift was at least as great as the subsidence caused by crustal thinning. Otherwise, the basement would have subsided below sealevel, resulting in sedimentation rather than the hiatus seen. The initial phase of rapid Eocene sedimentation and subsidence at Panyu 27-2-1 can be interpreted as a syn-rift episode, which was interrupted by a hiatus. The lack of initial post-rift subsidence is not predicted by a simple rift model but can be explained if Panyu 27-2-1, which is in the hanging wall of the first normal fault, was later uplifted due to motion on a second normal fault on which Panyu 27-2-1 is located in the footwall.

6. Discussion

6.1. Subsidence in Pearl River Mouth Basin

The combined seismic and well data allow us to limit major extension in the PRMB to prior to 25 Ma. Many of the wells show renewed, mild extension at 12–14 Ma, which may correlate in part with the observed reactivation of faults, disrupting the main post-rift sequences (Fig. 7). The amount of this extension ranges 3–8% ($\beta = 1.03 - 1.08$), based on uniform pure shear models (e.g. McKenzie, 1978) and does not significantly perturb the rate of post-rift subsidence. The even smaller and spatially limited extension event 4 seen at 5 Ma at Kaiping 1-1-1 and Panyu 33-1-1 also has little effect on the overall subsidence history, but can be related to a phase of dextral strike–slip shearing along this margin recognized by Chamot Rooke and Le Pichon (1999) and Wilson, Rais, Reigber, Reinhart, Ambrosius and Le Pichon (1999). This deformation appears to be related to motion the right-lateral Red River Fault and was initiated at this time, continuing to the present day, so explaining the slight deformation of very young sediments, or even the seafloor, around some faults (e.g. Fig. 7). This deformation does not generate significant accommodation space or sharply increase thermal subsidence rates across the basin and thus does not introduce significant errors into our subsidence calculations.

The identification of late stage motion on pre-existing faults seen in reflection seismic profiles confirms that some extension post-dated the main rift phase. Sedimentation in the central PRMB, and especially on the slope, was more rapid after 12 Ma, which could account for some of the observed basement subsidence, shown in the reconstructed histories. This is because the sediment can act as a load, depressing the margin landward of the depocentre. Although sediment loading at any given well is corrected for, apparent tectonic subsidence could occur if compensation was not perfectly local and isostatic and if the margin was loaded heavily on the slope. However, since flexural rigidity is low in South China, it is unlikely that such a load could depress the shelf to a significant extent. In any case, loading cannot account for the rapid steps in the reconstructed tectonic subsidence history. Rapid sedimentation after 12 Ma postdates the onset of enhanced subsidence at 14 Ma and pre-dates the event at 5 Ma, and would cause a gradual increase in subsidence as the size of the sediment load built up. This contrasts with the well-defined rapid steps in the subsidence history that could only be accounted for by a rapidly emplaced load or by tectonic extension.

Estimates of whole crust and mantle lithospheric extension prior to continental break-up across the South China Shelf are shown in Fig. 8. Several features of the deformation are noteworthy. The calculated extension of both crust and mantle increases towards the shelf edge, but is also high in the center of the PRMB, as sampled by Zhu-C, Zhu-5, Zhu-7 and Enping 12-1-1. Maximum whole crustal extension at any given place in the PRMB is estimated to be greater than 48%, based on the modeling of the reconstructed subsidence histories, as discussed above. This is compatible with an earlier study by Su et al. (1989), Westaway (1994) and Wheeler and White (1997) who estimated total crustal extension in the center of the PRMB of the South China Shelf to be 80%. Nissen et al. (1995a) obtained a similar value from seismic refraction data. On a regional scale, β_{crust} is typically smaller than β_{mantle}. This observation is an important clue that uniform pure extension is not operating in the formation of the South China margin, in contrast to the earlier conclusions of Su et al. (1989) and Wheeler and White (1997). At the simplest level, our result from the one dimensional backstripping on the South China Shelf would be compatible with the location of this area on the upper plate of a simple shear system, but could be caused by depth dependent extension of the style proposed by Driscoll and Karner (1998).

The continuation of continental extension to 25 Ma after the onset of seafloor spreading at 30 Ma along the South China Margin is an important new observation. It has a direct analogue in the Woodlark Basin of the Solomon Islands where active extension continues after the passage of the well-defined spreading axis (Goodliffe, Taylor, & Martinez, 1999; Mutter, Mutter, & Fang, 1996). In this area, extension is also affecting a region that had been an active magmatic arc in the recent past, and is flexurally weak. Such a situation is not known in rifts located within strong cratonic crust, such as the Red Sea, whose margins are too strong to distribute strain over broad areas, but which favor focusing this along spreading axes.

6.2. Subsidence in Beibu Gulf

Wells from the Beibu Gulf show different subsidence histories to those in the main part of the South China Shelf. Based on the dates of Su et al. (1989), the extension near these wells pre-dates that on the South China Shelf. Although the onset of rifting is not well defined, the end of rifting interpreted from a decrease in the rate of basement subsidence seen at Bei-B is much older (~43 Ma) than the estimate for the wells on the shelf. At each of the Beibu wells, the inferred crust and mantle extension are approximately similar, suggesting that a uniform mode of extension was operational in this region. Extension lasted for ~15 m.y. and resulted in 30–37% of extension ($\beta = 1.30$–1.37), less than the highest extension factors seen in the central PRMB.

7. Conclusions

The principle conclusion of the backstripping study undertaken here is that in the PRMB mantle extension exceeded crustal extension prior to the onset of seafloor spreading. However, the same is not true of the Beibu Gulf Basin, where extension is closer to being uniform.

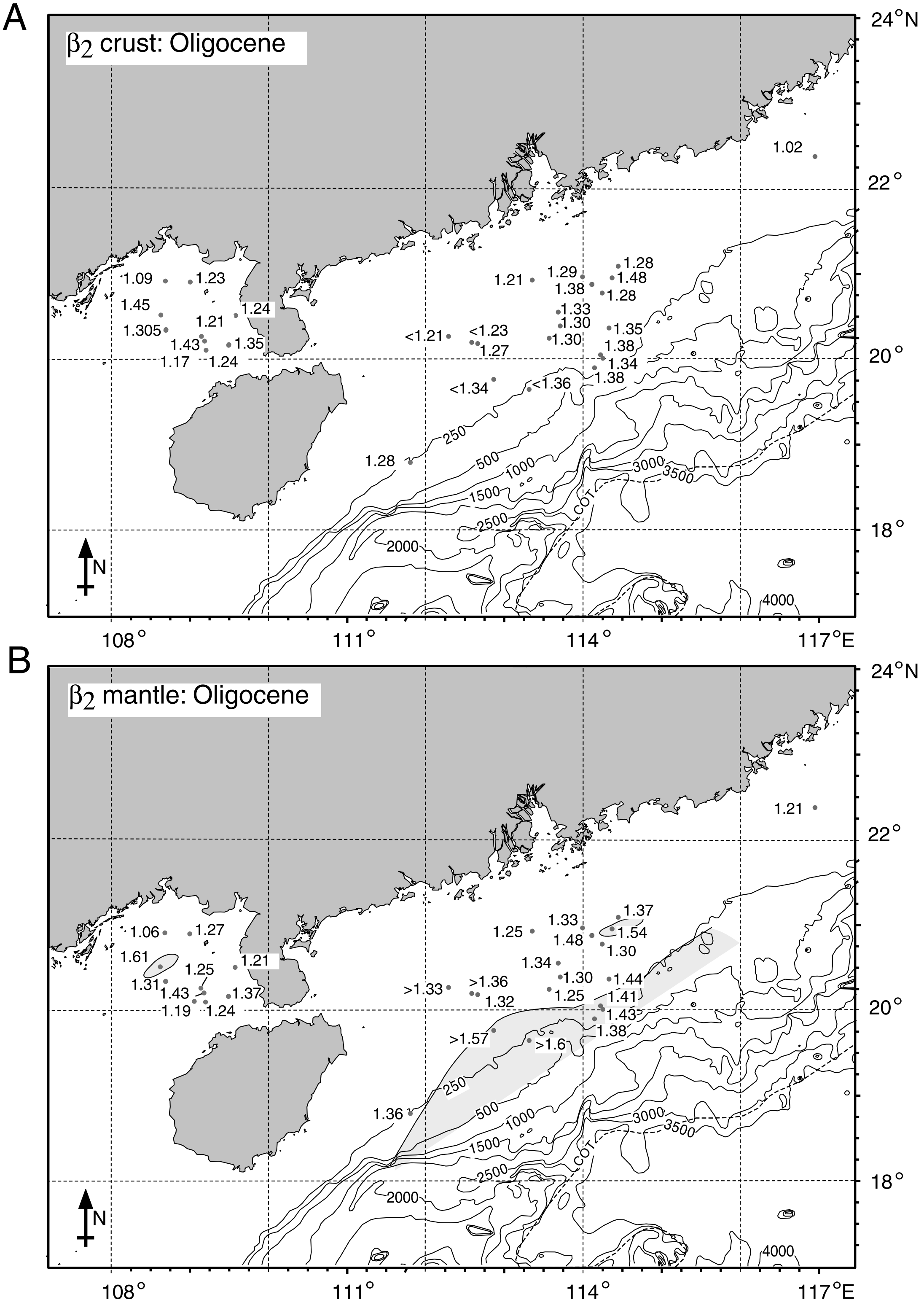

Fig. 8. (A) Map showing variations in crustal extension determined from one-dimensional backstripping of wells in the PRMB, immediately prior to the onset of seafloor spreading at 30 Ma. (B) Variations in mantle extension (β) derived from the observed rates of thermal subsidence since 28 Ma.

This pattern suggests that the mode of extension during intra-continental extension is different from that operating during continental break-up. A similar study would be required on the conjugate Palawan–Dangerous Grounds margin would be needed to demonstrate that a simple shear system, of which the PRMB formed the upper plate, was not operating here. However, although they are not the same magnitude, it is noteworthy that there is a correlation between increasing and decreasing mantle and crustal extension. This pattern is not compatible with a simple detachment system, but is more suggestive of a depth-dependent extension mechanism. The apparent uniform preferential loss of lower crustal material on both sides of the Nan Con Som Basin located ahead of the propagating rift tip in the SW corner of the basin (Fig. 1) further argues against the application of a simple shear model to this system (Clift et al., 2001)

The good agreement between crustal extension estimates derived from seismic refraction studies in the PRMB supports our conclusions and furthermore indicates that the local isostatic compensation assumption must be close to being correct in this area.

Early Paleocene rifting is documented in the Beibu Gulf and the PRMB, but is followed by stronger Oligocene extension in the latter prior to continental break-up. The timing of rifting is poorly constrained over much of the basin (~45–25 Ma) and makes a detailed and convincing correlation with either the poorly dated age of India–Asia collision (Rowley, 1996) or the onset of strike–slip faulting along the Red River Fault (e.g. Harrison et al., 1996) impossible.

Acknowledgements

The data used in this study was released by an agreement with the Chinese National Offshore Oil Company (CNOOC), and BP Amoco Exploration Operating Company Ltd. We are grateful to Richard Miller and David Roberts at BP Amoco for their generous help in providing data forthis study. This work was supported by the US Naval Oceanographic Office, Office of Naval Research, National Science Foundation and the Woods Hole Oceanographic Institution. This is WHOI contribution number 10484.

References

Barton, P., & Wood, R. (1984). Tectonic evolution of the North Sea Basin: Crustal stretching and subsidence. *Geophysical Journal of the Royal Astronomical Society*, *79*, 987–1022.

Berggren, W. A., Kent, D. V., Swisher, C. C., & Aubry, M. P. A. (1995). Revised Cenozoic geochronology and chronostratigraphy. *Geochronology, time scales and global stratigraphic correlation*. W. A. Berggren, D. V. Kent, M. P. Aubry & J. Hardenbol. *Society of Economic Paleontologists and Mineralogists Special Publication*, *54*, 129–212.

Boillot, G., Beslier, M. O., Krawczyk, C. M., Rappin, D., & Reston, T. J. (1995). The formation of passive margins: Constraints from the crustal structure and segmentation of the deep Galicia margin, Spain. *The tectonics, sedimentation and palaeoceanography of the North Atlantic region*. R. A. Scrutton, M. S. Stoker, G. B. Shimmield & A. W. Tudhope (Eds.), *Geological Society of London, Special Publication*, *Vol. 90*, (pp.71–91).

Briais, A., Patriat, P., & Tapponnier, P. (1993). Updated interpretation of magnetic anomalies and seafloor spreading stages in the South China Sea: Implication for the Tertiary tectonics of southeast Asia. *Journal of Geophysical Research*, *98*, 6299–6328.

Burchfiel, B. C., Royden, L. H., Wang, E., King, R., Chen, Z., Liu, Y., Zhang, Z., & Zhao, Z. (1997). Cenozoic tectonic evolution around the eastern Himalayan syntaxis. *Eos Transactions American Geophysical Union*, *78* (Fall Meeting Supplement), F173.

Chamot-Rooke, N., & Le Pichon, X. (1999). GPS determined eastward Sundaland motion with respect to Eurasia confirmed by earthquakes slip vectors at Sunda and Philippine trenches. *Earth and Planetary Science Letters*, *173*, 439–455.

Clift, P. D., & Turner, J. (1998). Paleogene igneous underplating and subsidence anomalies in the Rockall-Faeroe-Shetland area. *Marine and Petroleum Geology*, *15*, 223–243.

Clift, P. D., Clark, M. K., Royden, L. H., Burchfiel, B. C., & Whipple, K. X. (2000). Evolving sedimentary provenance in the Marginal Basins of South and East Asia. *Eos Transactions American Geophysical Union*, *81* (W. Pacific Meeting Supplement), 200.

Clift, P. D., Lin, J., & ODP Leg 184 Scientific Party (2001). Patterns of extension and magmatism along the continent–ocean boundary, South China margin. *Non-volcanic rifting of continental margins: A comparison of evidence from land and sea*. R. C. Wilson, R. B. Whitmarsh, B. Taylor & N. Froitzheim. *Geological Society of London, Special Publication*, in press.

Cung, T. C., Dorobek, S., Richter, C., Flower, M., Kikawa, E., Nguyen, Y. T., & McCabe, R. (1998). Paleomagnetism of Late Neogene basalts in Vietnam and Thailand: Implications for the post-Miocene tectonic history of Indochina. *Mantle dynamics and plate interactions in East Asia*. M. F. J. Flower, S.-L. Chung, C.-H. Lo & T. Y. Lee. *American Geophysical Union, Geodynamic Series*, *27*, 289–299.

Davis, D. W., Sewell, R. J., & Campbell, S. D. G. (1997). U–Pb dating of Mesozoic igneous rocks from Hong Kong. *Journal of the Geological Society, London*, *154*, 1067–1076.

Driscoll, N. W., & Karner, G. D. (1998). Lower crustal extension across the Northern Carnarvon basin, Australia: Evidence for an eastward dipping detachment. *Journal of Geophysical Research*, *103*, 4975–4991.

Ebinger, C. J., Bechtel, T. D., Forsyth, D. W., & Bowin, C. O. (1989). Effective elastic plate thickness beneath the East African and Afar plateaus and dynamic compensation of the uplifts. *Journal of Geophysical Research*, *94*, 2883–2901.

Eldholm, O., Skogseid, J., Planke, S., & Gladczenko, T. (1995). Volcanic margin concepts. In E. Banda, *Rifted ocean–continent boundaries*, E. Banda, M. Torné & M. Talwani (Eds.), (pp. 1–16). Dordrecht: Kluwer Academic Publishers.

Falvey, D., & Middleton, M. F. (1981). Passive continental margins: Evidence for a pre-breakup deep crustal metamorphic subsidence mechanism. *Colloquium on Geology of Continental Margins, Oceanologica Acta*, *4*, 103–114.

Foster, A. N., & Jackson, J. A. (1998). Source parameters of large African earthquakes; implications for crustal rheology and regional kinematics. *Geophysical Journal International*, *134* (2), 422–448.

Goodliffe, A. M., Taylor, B., & Martinez, F. (1999). Data report; marine geophysical surveys of the Woodlark Basin region. *Proceedings of the Ocean Drilling Program, Initial Reports*, *180*, 20.

Haq, B. U., Hardenbol, J., & Vail, P. R. (1987). Chronology of fluctuating sea levels since the Triassic. *Science*, *235*, 1156–1167.

Hamilton, W. (1979). *Tectonics of the Indonesian region*, *Geological Survey Paper #1087*. Washington DC: US Government Printing Office, pp. 1–345.

Harrison, T. M., Leloup, P. H., Ryerson, F. J., Tapponnier, P., Lacassin, R., & Wenji, C. (1996). Diachronous initiation of transtension along the Ailao Shan-Red River shear zone, Yunnan, Vietnam. In A. Yin & T. M. Harrison, *The tectonic evolution of Asia* (pp. 110–137). Cambridge: Cambridge University Press.

Hirth, G., & Kohlstedt, D. L. (1996). Water in the oceanic upper mantle; implications for rheology, melt extraction and the evolution of the lithosphere. *Earth and Planetary Science Letters*, *144* (1–2), 93–108.

Holloway, N. H. (1982). North Palawan Block, Philippines — its relation to Asian mainland and role in evolution of South China Sea. *American Association of Petroleum Geologists Bulletin*, *66*, 1355–1383.

Jahn, B., Chen, P. Y., & Yen, T. P. (1976). Rb–Sr ages of granitic rocks from southeastern China and their tectonic significance. *Geological Society of America Bulletin*, *87*, 763–776.

Jarvis, G. T., & McKenzie, D. P. (1980). The development of sedimentary basins with finite extension rates. *Earth and Planetary Science Letters*, *48*, 42–52.

Joy, A. M. (1992). Right place, wrong time: anomalous post-rift subsidence in sedimentary basins around the North Atlantic Ocean. *Magmatism and the causes of continental break-up*. B. C. Storey, T. Alabaster & R. J. Pankhurst (Eds.), *Geological Society of London, Special Publication*, *vol. 68*, (pp.387–393).

Karner, G. D., & Watts, A. B. (1982). On isostasy at Atlantic-type continental margins. *Journal of Geophysical Research*, *87*, 2923–2948.

Kelemen, P. B., & Holbrook, W. S. (1995). Origin of thick high-velocity igneous crust along the US east coast margin. *Journal of Geophysical Research*, *100*, 10077–10094.

Krawczyk, C. M., & Reston, T. J. (1995). Detachment faulting and continental break-up: The S reflector offshore Galicia. In E. Banda, M. Torné & M. Talwani, (Eds.), *Rifted ocean–continent boundaries* (pp. 231–245). Dordrecht: Kluwer Academic Publishers.

Kusznir, N. J., & Egan, S. S. (1989). Simple-shear and pure-shear models of extensional sedimentary basin formation: Application to the Jean d'Arc basin, Grand Banks of Newfoundland. *Extensional tectonics and stratigraphy of the North Atlantic margins*. A. J. Tankard & H. R. Balkwill. *American Association of Petroleum Geologists, Memoir*, *46*, 305–322.

Lee, T. Y., Lo, C. H., Chung, S. L., Lan, C. Y., Wang, P. L., & Lee, J. C. (1999). Cenozoic tectonics of the South China continental margins and the opening of the South China Sea. *Eos Transactions American Geophysical Union*, *80* (Fall Meeting Supplement), 1042.

Leloup, P. H., Harrison, T. M., Ryerson, F. J., Chen, W., Li, Q., Tapponnier, P., & Lacassin, R. (1993). Structural, petrological and thermal evolution of a Tertiary ductile strike–slip shear zone, Diancang Shan, Yunnan. *Journal of Geophysical Research*, *98*, 6715–6743.

Liu, Z., Wang, Q., Yuan, H., & Su, D. (1985). The Bouger anomalies and depths of Mohorovicic discontinuity in the South China Sea region. *Acta Oceanologica Sinica*, *4*, 579–590.

Lithgow-Bertelloni, C., & Gurnis, M. (1997). Cenozoic subsidence and uplift of continents from time-varying dynamic topography. *Geology*, *25*, 735–738.

Lu, W., Ke, C., Wu, J., Liu, J., & Lin, C. (1987). Characteristics of magnetic lineations and tectonic evolution of the South China Sea basin. *Acta Oceanologica Sinica*, *6*, 577–588.

Maggi, A., Jackson, J. A., McKenzie, D., & Priestley, K. (2000). Earthquake focal depths, effective elastic thickness, and the strength of the continental lithosphere. *Geology*, *28*, 495–498.

McKenzie, D. P. (1978). Some remarks on the development of sedimentary basins. *Earth and Planetary Science Letters*, *40*, 25–32.

Miller, K. G., Mountain, G. S., & Tucholke, B. E. (1985). Oligocene glacioeustacy and erosion on the margins of the North Atlantic. *Geology*, *13*, 10–13.

Mutter, J. C., Mutter, C. Z., & Fang, J. (1996). Analogies to oceanic behaviour in the continental breakup of the western Woodlark Basin. *Nature*, *380*, 333–336.

Nissen, S. S., Hayes, D. E., Buhl, P., Diebold, J., Bochu, Y., Weijun, Z., & Yongqin, C. (1995a). Deep penetration seismic soundings across the northern margin of the South China sea. *Journal of Geophysical Research*, *100*, 22407–22433.

Nissen, S. S., Hayes, D. E., Bochu, Y., Weijun, Z., Yongqin, C., & Xiaupin, N. (1995b). Gravity, heat flow, and seismic constraints on the processes of crustal extension: Northern margin of the South China sea. *Journal of Geophysical Research*, *100*, 22447–22483.

Packham, G. (1996). Cenozoic SE Asia: Reconstructing its aggregation and reorganization. *Tectonic evolution of Southeast Asia*. R. Hall & D. Blundell. *Geological Society of London, Special Publication*, *106*, 123–152.

Peltzer, G., & Tapponnier, P. (1988). Formation and evolution of strike–slip faults, rifts, and basins during the India–Asia collision: An experimental approach. *Journal of Geophysical Research*, *93*, 15085–15117.

Petit, C., & Ebinger, C. (2000). Flexure and mechanical behavior of cratonic lithosphere; gravity models of the East African and Baikal rifts. *Journal of Geophysical Research*, *105*, 19151–19162.

Reston, T. J., Krawczyk, C. M., & Hoffman, H. -J. (1995). Detachment tectonics during Atlantic rifting: analysis and interpretation of the S reflection, the west Galicia margin. *The tectonics, sedimentation and palaeoceanography of the North Atlantic region*. R. A. Scrutton, M. S. Stoker, G. B. Shimmield, & A. W. Tudhope, (Eds.), *Geological Society of London, Special Publication*, *vol. 90*, (pp.93–109).

Rowley, D. B. (1996). Age of initiation of collision between India and Asia; a review of stratigraphic data. *Earth and Planetary Science Letters*, *145*, 1–13.

Royden, L., & Keen, C. E. (1980). Rifting processes and thermal evolution of the continental margin of eastern Canada determined from subsidence curves. *Earth and Planetary Science Letters*, *51*, 714–717.

Sawyer, D. (1986). Effect of basement topography on subsidence history analysis. *Earth and Planetary Science Letters*, *78*, 427–434.

Sibuet, J. C., Louvel, V., Whitmarsh, R. B., White, R. S., Horsefield, S. J., Sichler, B., Leon, P., & Recq, M. (1995). Constraints on rifting processes from refraction and deep-tow magnetic data: the example of the Galicia continental margin (west Iberia). In E. Banda, *Rifted ocean–continent boundaries* (pp. 197–217). Dordrecht: Kluwer Academic Publishers.

Schlüter, H. U., Hinz, K., & Block, M. (1996). Tectono-stratigraphic terranes and detachment faulting of the South China Sea and Sulu Sea. *Marine Geology*, *130*, 39–78.

Sclater, J. G., & Christie, P. A. F. (1980). Continental stretching: an explanation of the post Mid-Cretaceous subsidence of the central North Sea basin. *Journal of Geophysical Research*, *85*, 3711–3739.

Sewell, R. J., & Campbell, S. D. G. (1997). Geochemistry of coeval Mesozoic plutonic and volcanic suites in Hong Kong. *Journal of Geological Society, London*, *154*, 1053–1066.

Steckler, M. S., Berthelot, F., Lyberis, N., & Le Pichon, X. (1988). Subsidence in the Gulf of Suez; implications for rifting and plate kinematics. *Tectonophysics*, *153*, 249–270.

Su, D., White, N., & McKenzie, D. (1989). Extension and subsidence of the Pearl River mouth basin, northern South China Sea. *Basin Research*, *2*, 205–222.

Tapponnier, P., Peltzer, G., & Armijo, R. (1986). On the mechanics of the collision between India and Asia. *Collision tectonics*. M. P. Coward & A. C. Ries. *Geological Society of London, Special Publication*, *19*, 115–157.

Taylor, B., & Hayes, D. E. (1980). The tectonic evolution of the South China Basin. *The tectonic and geologic evolution of Southeast Asian seas and islands*. D. E. Hayes. *American Geophysical Union, Geophysical Monograph*, *23*, 89–104.

Taylor, B., & Hayes, D. E. (1983). Origin and history of the South China Sea basin. *The tectonic and geologic evolution of Southeast Asian seas and islands; part 2*. D. E. Hayes. *American Geophysical Union, Geophysical Monograph*, *27*, 23–56.

Wang, P. L., Lo, C. H., Lee, T. Y., Chung, S. L., & Yem, N. T. (1998). Thermochronological evidence for the movement of the Ailao Shan-Red River shear zone: A perspective from Vietnam. *Geology*, *26*, 887–890.

Wang, P., Prell, W. L., Blum, P., Arnold, E. M., Buehring, C. J., Chen, M.-P., Clemens, S. C., Clift, P. D., Colin, C. J. G., Farrell, J. W., Higginson, M. J., Zhimin, J., Kuhnt, W., Laj, C. E., Lauer-Leredde, C., Leventhal, J. S., Li, A., Li, Q., Lin, J., McIntyre, K., Miranda, C. R., Nathan, S. A., Shyu, J.-P., Solheid, P. A., Su, X., Tamburini, F., Trentesaux, A. & Wang, L. (2000). *Proceedings of the Ocean Drilling Program, Initial Reports, 184*. College Station, TX: Ocean Drilling Program.

Watts, A. B., & Stewart, J. (1998). Gravity anomalies and segmentation of the continental margin offshore West Africa. *Earth and Planetary Science Letters*, *156*, 239–252.

Webb, T., (1992). *Extension and subsidence in the Beibu Gulf basin, South China Sea*. Unpublished M.Sc. Thesis, University of Texas at Dallas.

Wernicke, B. P. (1985). Uniform sense of normal simple shear of the continental lithosphere. *Canadian Journal of Earth Sciences*, *22*, 108–125.

Westaway, R. (1994). Re-evaluation of extension across the Pearl River mouth basin, South China Sea: Implications for continental lithosphere deformation mechanisms. *Journal of Structural Geology*, *16*, 823–838.

Wheeler, P. J., & White, N. J. (1997). Basin kinematics in South East Asia — tectonics and dynamic implications (abstract). *Eos Transactions, American Geophysical Union*, *78*, F658.

Wilson, P., Rais, J., Reigber, C., Reinhart, E., Ambrosius, B. A. C., Le Pichon, X., Kasser, M., Suharto, P., Majid, D.'A., Bin Haji, Y., Awang Haji Othman, Dato'Paduka, Almeda, R., & Boonphakdee, C. (1999). Study provides data on active plate tectonics in Southeast Asia region. *Eos Transactions American Geophysical Union*, *79* (Fall Meeting Supplement), 548–549.